Encoder Design for the Multiple Symbol Trellis Coded Modulation Applied to Noncoherent CPFSK on the Interleaved Rician Fading Channel

Chang-Joong Kim[1] and Ho-Kyoung Lee[2]
Department of Radio Communication Science and Engineering, Hong-Ik University,
Sangsoo-Dong 72-1, Mapo-gu, Seoul 121-791, Korea.
(Phone)+82-2-320-1485, (Fax)+82-2-320-1193
E-mail:[1]ga2314501@wow1.hongik.ac.kr, [2]hklee@wow.hongik.ac.kr

Abstract: In this paper, we introduce an encoder design technique of multiple symbol trellis coded modulation for noncoherent continuous phase frequency shift keying (MTCM/NCPFSK) on the interleaved Rician fading channel. To find dominant factors which affects the error probability of MTCM/NCPFSK, we derive the pairwise error probability (PEP) of MTCM/NCPFSK and find that the error probability mainly depends on the effective length of error event and the corresponding squared product distance (SPD) for the small value of Rician parameter K. Using this performance criteria, we search for the optimal encoder of MTCM/NCPFSK for the interleaved Rician fading channel. We also compare that encoder with the encoder designed for additive white Gaussian noise channel.

1. Introduction

Radio or satellite channels are power- and bandwidth-limited channels whose fading amplitudes are modeled as Rician or Rayleigh distributions. Power- and bandwidth-efficient coded modulation scheme such as trellis coded modulation applied to continuous phase modulation (TCM/CPM) combined with interleaving technique can be an appropriate solution for these channels [1]. Many researchers have studied the design technique of TCM/CPM [1], [2], [3], [4], [5], especially [5] presents a multiple symbol trellis coded modulation scheme applied to noncoherent continuous phase modulation (MTCM/NCPFSK) on the additive white Gaussian noise (AWGN) channel.

In this paper, we modify the design technique presented in [5] and apply that for the interleaved Rician fading channel with ideal channel state information. To reduce temporal correlation of channel, we insert an interleaver between trellis encoder and continuous phase modulator as the system presented in [1]. We derive the pairwise error probability (PEP) of MTCM/NCPFSK and find the union bound of the event error probability on the interleaved Rician fading channel. The optimal encoder is found for MTCM/NCPFSK by using the result of performance analysis. Computer simulations are also presented to verify the results.

2. System Model

Fig. 1 shows the block diagram of MTCM/NCPFSK system which has an interleaver and a deinterleaver. Input binary symbols b_m occurring at a rate R_b are passed through a trellis encoder with code rate r producing a sequence of encoded binary symbols c_m at a rate $R_s = R_b/r$. The encoded binary symbols c_m is mapped to N-consecutive M-ary symbols $\mathbf{a_m} = \left(a_{(m,0)}, a_{(m,1)}, \cdots, a_{(m,N-1)}\right)$, and $a_{(m,i)} \in \{0, 1, \cdots, M-1\}$. The sequence of $\mathbf{a_m}$ is interleaved by using N-consecutive symbol interleaver (NCSI). The continuous phase modulator is represented with N-consecutive continuous phase encoder (NCPE) and memoryless modulator (MM) as explained in [5]. The output of the NCPE is hence represented by the sequence $\{(\mathbf{a_m}, V_m)\}$, which is the input to the MM. The input vector $\mathbf{a_m}$ and the state of NCPE V_m determine the transmitted N-consecutive M-ary CPFSK waveform during the time interval $[mT_N, (m+1)T_N)$.

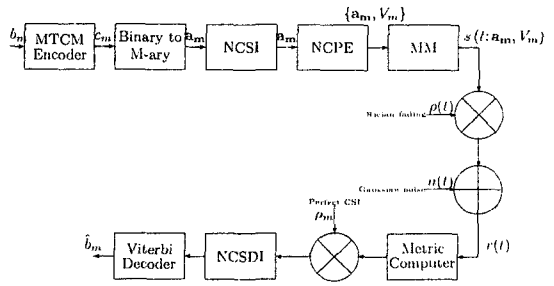

Figure 1. The Block Diagram of MTCM/NCPFSK System for Interleaved Fading Channel

During the time interval $[mT_N, (m+1)T_N)$, the complex baseband CPFSK waveform is, $s(t; \mathbf{a_m}, V_m) = \sqrt{\frac{2\varepsilon}{T}} e^{j\Psi(t;\mathbf{a_m}, V_m)}$, where ε is the symbol energy, T is the symbol duration, $T_N = TN$ is the N-consecutive symbol duration, and Ψ, the information carrying phase is expressed as

$$\Psi(t; \mathbf{a_m}, V_m) \triangleq 2\pi h \left(V_m + \sum_{k=0}^{i-1} a_{(m,k)} + a_{(m,i)} \frac{(\tau - iT)}{T} \right) \mod 2\pi, \quad \text{if } mT_N + iT \le t < mT_N + (i+1)T, \text{ for } i = 0, 1, \cdots N-1 \tag{1}$$

where the parameter h is referred as the modulation index. In this paper, we only consider the case of $h = 1/M$. To keep the phase constant, we express the next state as $V_{m+1} = V_m + \sum_{k=0}^{N-1} a_{(m,k)} \mod M$.

For a flat fading channel as modeled in Fig. 1, the complex baseband form of the received signal during the time interval $[mT_N, (m+1)T_N)$ is $r(t) = \rho(t) s(t; \mathbf{a_m}, V_m) e^{j\phi(t)} + n(t)$, where $n(t)$ is a zero-mean complex Gaussian random process with power spectral

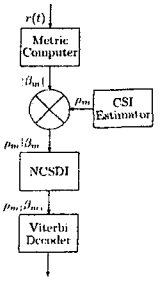

Figure 2. Maximum Likelihood Receiver Designed for Interleaved Rician Fading Channel

density N_0 W/Hz, $\rho(t)$ is a fading amplitude and $\phi(t)$ is an arbitrary phase offset. We assume that the channel is varying slow so that the fading gain $\rho(t)$ and the arbitrary phase offset $\phi(t)$ are constant values during the time interval $[mT_N, (m+1)T_N)$, i.e. $\rho(t) = \rho_m, \quad \phi(t) = \phi_m$. Since the receiver detects the received signal noncoherently, the phase states generated by the NCPE memory states V_m is not differentiated in the receiver. Hence we rewrite the received waveform during the time interval $[mT_N, (m+1)T_N)$ as

$$r(t) = \rho_m s(t; \mathbf{a_m}, 0) e^{j\theta_m} + n(t) \tag{2}$$

where $\theta_m = \phi_m + (2\pi h V_m \mod 2\pi)$ is the phase ambiguity at the receiver. The probability density function of ρ_m is assumed to be a Rician random variable, whose probability density function is given by

$$f_{\rho_m}(\rho) = 2\rho(1+K)e^{-K-\rho^2(1+K)} I_0(2\rho\sqrt{K(1+K)}) \tag{3}$$

where $I_0(\cdot)$ denotes the modified Bessel function of first kind and K is the Rician parameter.

3. Maximum Likelihood Receiver for Noncoherent Detection and Performance Analysis

In this section, we derive the maximum likelihood receiver with perfect channel state information based on the system model described in previous section for noncoherent detection. With the perfect interleaving, the sequence of the fading gain $\{\rho_m\}$ is modeled as an independent and identically distributed random sequence. Considering noncoherent detection and perfect channel state information, we derive the likelihood function,

$$\Lambda(r(t)|\mathbf{A_L}, \rho_\mathbf{L}) = \sum_{m=0}^{L-1} \rho_m |\beta_m| \tag{4}$$

where β_m is the complex cross-correlation given by $\beta_m = \int_{mT_N}^{(m+1)T_N} r(t) e^{-j\Psi(t;\mathbf{a_m},0)} dt$. Note that the cross-correlation β_m is independent to the phase ambiguity θ_m. The optimum detector of MTCM/NCPFSK is explained in Fig. 2. Metric computer calculate $|\beta_m|$ and $\rho_m|\beta_m|$ is the branch metric of Viterbi decoder. The receiver designed for interleaved Rician fading channel is similar to the receiver designed for AWGN in [5]. Thus, the receiver described in [5] is the special case of the receiver designed for interleaved Rician fading channel.

Using the log-likelihood function derived in (4), we obtain the conditional pairwise error probability(PEP) associated with the transmitted sequence $\mathbf{A_L}$ and the erroneous sequence $\hat{\mathbf{A}}_\mathbf{L}$ given the channel state information as

$$\Pr(\mathbf{A_L} \to \hat{\mathbf{A}}_\mathbf{L}|\rho_\mathbf{L}) = \Pr\left(\sum_{m=0}^{L-1} \rho_m|\beta_m| > \sum_{m=0}^{L-1} \rho_m|\hat{\beta}_m| \right) \tag{5}$$

where $\hat{\beta}_m$ is the erroneous complex correlation associated with the transmitted sequence $\hat{\mathbf{A}}_\mathbf{L}$. For the convenience, we denote Y as $Y = \sum_{m=0}^{L-1} \rho_m|\beta_m| - \sum_{m=0}^{L-1} \rho_m|\hat{\beta}_m|$. Using the linear approximation presented in [5], Y is approximated to the Gaussian random variable Y_a with mean $\mu_{Y_a} = AT\sum_{m=0}^{L-1} \rho_m^2(N - |\xi_m|)$ and variance $\sigma_{Y_a}^2 = N_0 T \sum_{m=0}^{L-1} \rho_m^2(N - |\xi_m|)$, where ξ_m denotes $\xi_m = \frac{1}{T}\int_{mT_N}^{(m+1)T_N} e^{j\Psi(t;\Delta\mathbf{a_m},0)} dt$ and $\Delta\mathbf{a_m} = \mathbf{a_m} - \hat{\mathbf{a}}_\mathbf{m}$. Thus, the conditional PEP is approximated as below

$$\Pr(\mathbf{A_L} \to \hat{\mathbf{A}}_\mathbf{L}|\rho_\mathbf{L}) \approx Q\left(\sqrt{\frac{\bar{\varepsilon}}{2N_0} \sum_{m\in\eta} \rho_m^2 d_{e,m}^2} \right) \tag{6}$$

where $Q(\cdot)$ is the Gaussian integral function, η denotes the set of the time index m which makes $\Delta\mathbf{a_m} \neq 0$, and $d_{e,m}^2 = 2(N - |\xi_m|)$.

We average the conditional PEP over $\rho_\mathbf{L}$ to obtain the PEP. Using moment generating function(MGF) method and Gauss-Chebysev quadrature in [11] we derive the PEP,

$$\Pr(\mathbf{A_L} \to \hat{\mathbf{A}}_\mathbf{L}) = \frac{1}{2k} \sum_{j=1}^{k} \prod_{m\in\eta} \frac{1+K}{1+K+\delta_{mj}^2} \exp\left(-\frac{K\delta_{mj}^2}{1+K+\delta_{mj}^2} \right) + R_k \tag{7}$$

where $\delta_{mj}^2 \triangleq \left[\bar{\varepsilon} d_{e,m}^2 \sec^2\left[(2j-1)\pi/4k\right]\right]/4N_0$ and R_k is the remainder term. As k increases the remainder term R_m becomes negligible, as demonstrated by [11]. When the channel tends towards Rayleigh fading channel and E_b/N_0 is high enough, the PEP is simplified as

$$\begin{aligned} &\Pr(\mathbf{A_L} \to \hat{\mathbf{A}}_\mathbf{L}) \\ &< \frac{1}{2k} \sum_{j=1}^{k} \prod_{m\in\eta} \frac{1+K}{\delta_{mj}^2} e^{-K} + R_k \\ &= \frac{1}{2k} \sum_{j=1}^{k} \left[\frac{C_j(1+K)e^{-K}}{\gamma_4} \right]^{l_\eta} \frac{1}{d_p^2(l_\eta)} + R_k \end{aligned} \tag{8}$$

where $\gamma_4 = \bar{\varepsilon}/4N_0$, $C_j = \cos^2\left[(2j-1)\pi/4k\right]$, $d_p^2(l_\eta) = \prod_{m\in\eta} 1/d_{e,m}^2$, and l_η is the effective length, the number of elements in the set η. From (8), we observe that the PEP is inversely proportional to the squared product distance, $d_p^2(l_\eta)$ and the l_ηth power of the SNR. The PEP mainly depends on the effective length l_η and the corresponding squared product distance.

By summing the PEP at high SNR obtained in equation (8), we construct the union bound of the bit error probability at high SNR as below

$$P_b \leq \frac{1}{b} \sum_{l_\eta} \sum_{d_p^2(l_\eta)} w\left(l_\eta, d_p^2(l_\eta)\right) \left[\frac{1}{2k} \sum_{j=1}^{k} \left[\frac{C_j(1+K)e^{-K}}{\gamma_4} \right]^{l_\eta} \frac{1}{d_p^2(l_\eta)} + R_k \right] \quad (9)$$

where b is the number of trellis encoder input bits, $w(l_\eta, d_p^2(l_\eta))$ is the average hamming distance of code sequences having the effective length l_η and the squared product distance $d_p^2(l_\eta)$. Among all terms in (9) the one with the smallest effective length l_η and the smallest product distance $d_p^2(l_\eta)$ dominates the bit error probability at high SNR. Denoting $min(l_\eta)$ by L and the corresponding squared product distance by $d_p^2(L)$, the error event probability is asymptotically approximated as

$$P_b \approx \frac{1}{b} w\left(L, d_p^2(L)\right) \left[\frac{1}{2k} \sum_{j=1}^{k} \left[\frac{C_j(1+K)e^{-K}}{\gamma_4} \right]^{L} \frac{1}{d_p^2(L)} + R_k \right] \quad (10)$$

Therefore, for small values of K and large values of γ_4, the bit error probability P_b is determined by the parameters such as the minimum effective length L, and the corresponding squared product distance $d_p^2(L)$.

4. Optimal Trellis Encoder Design for Small Values of Rician Parameter K

4.1 Encoder design

Considering equation (10), for small values of K, in other words when the channel tends toward Rayleigh, the optimal trellis encoder maximizes the minimum effective length L, and the corresponding squared product distance $d_p^2(L)$. These design criteria are quite different from the optimal trellis encoder design criteria for AWGN channel. We search the optimal trellis encoder when the channel tends towards Rayleigh using L and $d_p^2(L)$ as the primary design criteria and the equivalent squared free distance $d_{e,free}^2$ defined in [5] as the secondary design criterion. We consider a binary convolutional encoder with code rate $r = 3/4$ cascaded to the 2-consecutive 4-ary NCPE. We implement this convolutional encoder using the general encoder implementation scheme of [5]. The set partitioning condition in [5] decides the values of h_0^i's. An exhaustive search to find the remaining coefficients to maximize primarily the minimum effective length L and the corresponding squared product distance $d_p^2(L)$ and secondarily the equivalent squared free distance $d_{e,free}^2$ has been performed. We modified the computational algorithm in [13] to search good encoders for interleaved Rician fading channel.

We represent the $[h^3, \cdots, h^1, h^0]$ in the octal representation in the same way shown in [14]. Comparing Table 1 with results of [5], we observe that two encoders

# of states	ν	h_3	h_2	h_1	h_0	L	$d_p^2(L)$	$d_{e,free}^2$
2	1	0	2	0	1	1	1.453521	0.975689
4	2	0	2	4	1	1	1.629106	0.975689
8	3	2	10	4	3	2	0.562460	1.374424
16	4	4	12	2	21	2	1.675837	1.374424

Table 1. Optimal Code Rate 3/4 Trellis Encoder Cascaded to 2CPE with M=4 for Interleaved Rician Fading Channel

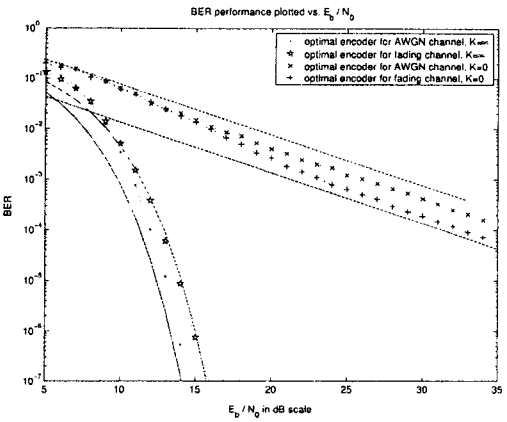

Figure 3. Bit Error Rate Plotted versus $E_b/N_0(dB)$ for Various Values of K with the Optimal Encoder for $K = 0$ and the Optimal Encoder for $K = \infty$ with $\nu = 2$

are same for the case of $\nu = 1$, but for the other cases, they are different.

4.2 Computer simulations and discussions

In this subsection, we show simulation and analytically approximated results of bit error probability. We use the equation (10) to get an approximation on the bit-error probability. The approximated bit error rate may be smaller than the simulated value because the equation (10) is evaluated by using only the most dominant term of the union bound on the bit error probability.

Fig. 3 and Fig. 4 show that the logarithm of bit error rate is decreasing linearly for Rician fading channel, while it is decreasing exponentially for AWGN channel. It results from the fact that the bit error probability is given by the equation (10) for small values of K, while it is given by Q function for $K = \infty$.

Fig. 3 shows the performance of the system using the optimal code rate 3/4 trellis encoders cascaded to 2 CPE with $M = 4$, $h = 1/4$, and $\nu = 2$. For small values of K, we observe that the logarithm of the bit error probability of the optimal encoder for Rician fading channel and that for AWGN channel are decreasing linearly with almost same slope. But as SNR increases, for small values of K, the performance of the optimal encoder designed for Rician fading channel becomes better than the optimal encoder designed for AWGN channel. This result come from the reason that the effective lengths of two encoders are same and the corresponding squared distances for them are different.

Fig. 4 shows the performance of the system using the optimal code rate 3/4 trellis encoders cascaded to 2

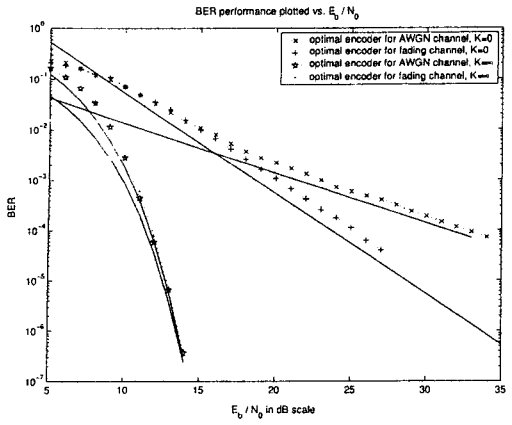

Figure 4. Bit Error Rate Plotted versus $E_b/N_0(dB)$ for Various Values of K with the Optimal Encoder for $K = 0$ and the Optimal Encoder for $K = \infty$ with $\nu = 3$

CPE with $M = 4$, $h = 1/4$, and $\nu = 3$. In this case, for small values of K, we observe that the logarithm of the bit error probability of the optimal encoder for Rician fading channel and AWGN is plotted as straight lines with the slope values 2 and 1 respectively. Theses results come from the fact that the effective length of the optimal encoder for Rician fading channel is 2 while that for AWGN channel is 1. Thus, for the small values of K, as SNR increases, the performance difference becomes large. However, for the large values of K, we observe that the performance difference between two encoders is negligible.

5. Conclusion

We find the performance criteria of MTCM/NCPFSK with noncoherent detection for interleaved Rician fading channel and designed the optimal trellis encoder for interleaved Rician fading channel using the performance criteria.

By the result of performance analysis, for small values of K, we observed that the error performance of the system is inverse proportion to the Lth power of the SNR and the corresponding squared product distance $d_p^2(L)$ while, for large values of K, the error performance of the system depends on the equivalent squared free distance $d_{e,free}^2$. It is same to the case of trellis coded M-ary phase shift keying(TC-MPSK) described in [7], [8]. In the other words, the same parameters which affect the performance of TC-MPSK affect the performance of our system. We designed the optimal encoder for interleaved Rician fading channel by using these parameters. Simulations have been performed to verify the performance analysis and the encoder design criteria.

By the result of analysis and simulation, we observed that the optimal encoder for AWGN channel is not always optimum for interleaved Rician fading channel. Mobile or radio channels are fading channels as well as power- and bandwidth- limited channels. Therefore, in such channel environment, the optimal encoder for interleaved Rician channel is better than the optimal encoder for AWGN channel.

References

[1] F. Abrishamkar, E. Biglieri, "Suboptimum detection of trellis-coded CPM for transmission on bandwidth- and power limited channels," *IEEE Trans. Commun.*, vol. 39, pp. 1065–1074, July 1991.

[2] R. W. Kerr and P. J. McLane, "Coherent detection of interleaved trellis encoded CPFSK on shadowed mobile satellite channels," *IEEE Trans. Veh. Technol.*, vol. 41., pp.159–169, May 1992.

[3] L. Yiin and G. L. Stüber, "Error probability of coherent detection for trellis-coded partial response CPM on Rician-fading channels," in *IEEE Global Telecommun. Conf.*, San Francisco, CA, Nov. 1994, pp. 359–363.

[4] L. Yiin and G. L. Stüber, "Noncoherently detected trellis-coded partial response CPM on mobile radio channels," *IEEE Trans. Commun.*, vol. 44, pp. 967–975, Aug. 1996.

[5] H. K. Lee, "Multiple-symbol trellis-coded modulation applied to noncoherent continuous-phase frequency shift keying," *IEEE Trans. Inform. Theory*, vol. 43, pp. 454–468, Mar. 1997.

[6] B. Rimoldi, "A decomposition approach to CPM," *IEEE Trans. Inform. Theory*, vol 34., no. 2, pp.260–270, Mar. 1988.

[7] D. Divsalar and M. K. Simon, "Trellis-coded modulation for 4800 to 9600 bps transmission over a fading satellite channel," *IEEE J. Select. Areas. Commun.*, vol. 5, pp. 162–175, Feb. 1987.

[8] D. Divsalar and M. K. Simon, "The design of trellis coded MPSK for fading channels: performance criteria," *IEEE Trans. Commun.*, vol. 36, pp. 1004–1011, Sept. 1988.

[9] S. B. Slimane and Tho Le–Ngoc, "Tight bounds on the error probability of coded modulation schemes in Rayleigh fading channels," *IEEE Trans. Veh. Technol.*, vol. 44, no.1, pp. 121–129, Jan. 1995.

[10] S. B. Slimane and Tho Le–Ngoc, "A tight upper bound on the error probability of coded modulation schemes in Rayleigh fading channels," in *PIMRC'93*, Yokohama, Japan, pp. 249–253, Sept. 1993.

[11] C, Tellambura, "Evaluation of the exact union bound for trellis-coded modulations over fading channels," *IEEE Trans. Commun.*, vol.44, pp. 1693–1699, Dec. 1996.

[12] C. Schelgel and D. J. Costello, Jr., "Bandwidth efficient coding for fading channels: code construction and performance analysis," *IEEE J. Select. Areas. Commun.*, vol. SAC–5, pp. 162–175, Feb. 1987.

[13] I. Biglieri, D. Divsalar, P. McLane, and M. Simon, *Introduction to Trellis-Coded Modulation with Application.* New York: Macmillan, 1991.

[14] S. S. Pietrobon, R. H. Deng, A. Lafanechére, G. Ungerboeck, and D. J. Costello. Jr., "Trellis-coded multidimensional phase modulation," *IEEE Trans. Inform. Theory*, vol. 36, no. 1, pp 63–89, Jan. 1990.